Young's Modulus Determination of Normal and Glaucomatous Human Iris

Arun Narayanaswamy,[1] Mui Hoon Nai,[2] Monisha E. Nongpiur,[1,3] Hla Myint Htoon,[1,3] Anoop Thomas,[4] Tiakumzuk Sangtam,[4] Chwee Teck Lim,[2,5,6] Tina T. Wong,[1,3] and Tin Aung[1,3,7]

[1]Singapore Eye Research Institute and Singapore National Eye Center, Singapore
[2]Department of Biomedical Engineering, National University of Singapore, Singapore
[3]Duke-NUS Graduate Medical School, Singapore
[4]Department of Ophthalmology & Visual Sciences Khoo Teck Puat Hospital, Singapore
[5]Mechanobiology Institute, National University of Singapore, Singapore
[6]Biomedical Institute for Global Health Research and Technology, National University of Singapore, Singapore
[7]Yong Loo Lin School of Medicine, National University of Singapore, Singapore

Correspondence: Arun Narayanaswamy, Singapore National Eye Center, 11 Third Hospital Avenue, Singapore 168751, Singapore; answamy22@gmail.com.

AN and MHN contributed equally to the work presented here and should therefore be regarded as equivalent authors.

Submitted: December 15, 2018
Accepted: May 7, 2019

Citation: Narayanaswamy A, Nai MH, Nongpiur ME, et al. Young's modulus determination of normal and glaucomatous human iris. *Invest Ophthalmol Vis Sci*. 2019;60:2690–2695. https://doi.org/10.1167/iovs.18-26455

Purpose. To evaluate the biomechanical properties (Young's modulus) of normal (control) and glaucomatous human iris using atomic force microscopy (AFM).

Methods. Iris tissue obtained from eighteen glaucomatous subjects (equal number of eyes with primary angle closure glaucoma (PACG) and primary open angle glaucoma (POAG) and five normal subjects who underwent elective eye surgery were subjected to the estimation of Young's modulus by AFM. Force measurements were done at room temperature using Nanowizard II BioAFM. The iris samples were immersed in the liquid media (PBS with 0.1% BSA) during force measurements. Young's modulus values were calculated for each recorded curve using JPK Data Processing Software, which uses a Hertz's contact model for spherical indenters fitted to the extend curves.

Results. The iris from the normal controls had the least Young's modulus (0.85 ± 0.31 kPa) while those from PACG patients had the highest Young's modulus (2.40 ± 0.82 kPa). The Young's modulus of PACG iris was significantly higher compared to that of the normal controls ($P = 0.005$) and POAG iris ($P = 0.001$). However, there was no significant difference in the Young's modulus of POAG iris (1.13 ± 0.36 kPa) compared to that of the normal controls ($P = 0.511$).

Conclusions. Variations in biomechanical properties of iris tissue may have a significant role in the pathogenesis of angle closure glaucoma. This study suggests the existence of fundamental biomechanical differences in eyes with angle closure versus open angle glaucoma. An understanding of this basis creates a new platform to understand disease pathology better and work on therapeutic strategies that will address the same.

Keywords: iris, angle closure, AFM, glaucoma, ocular biomechanics, stiffness

Primary angle closure and primary angle closure glaucoma (PACG) occur more commonly in eyes with shorter axial length (AL), shallower anterior chamber (AC), and a relatively larger lens.[1–4] However, anatomic features alone do not adequately explain why many people with small eyes and narrow angles never develop the disease.[1] It is likely that static measurements overlook the dynamic physiologic changes in ocular structures, such as the iris and choroid. These changes and their relationship with other structures, such as the lens may determine the status of the angle width at a given point in time.

The iris in eyes with PACG differs from those without disease.[5–7] Some variations may be attributed to differences in their biomechanical properties, since the iris is predominantly composed of collagen, extracellular matrix proteins, and smooth muscle fibers.[8,9] Indentation using atomic force microscopy (AFM) is evolving as a powerful tool for studying the local micromechanical properties of a variety of biological tissues, cells, and biomaterials.[10–12] AFM allows mapping of the spatial distribution and provides a quantitative measurement of the Young's modulus of the iris tissue. Young's modulus is a measure of a solid's stiffness or resistance to elastic deformation under load. The basic principle is that a material undergoes elastic deformation when it is compressed or extended, returning to its original shape when the load is removed. More deformation occurs in a compliant material (lower Young's modulus) compared to that of a stiff material.[13] An in-depth evaluation of these iridial properties may provide significant insights into the pathogenesis and management of angle closure disease.

This study was designed to specifically evaluate and understand the biomechanical properties of the iris that could provide an insight to the pathogenesis of PACG.

Methods

Approval for the study was granted by the Singapore Eye Research Institute institutional review board. This study was conducted in accordance with the Declaration of Helsinki, and

written informed consent was obtained from all subjects before enrollment.

This was a comparative study of subjects with PACG, primary open angle glaucoma (POAG), and normals recruited from clinics at the Singapore National Eye Centre and Khoo Teck Puat Hospital, Singapore. All subjects were of Chinese descent and were scheduled for an elective eye surgery (trabeculectomy/phaco-trabeculectomy or extracapsular cataract extraction). They underwent a standardized eye examination that included visual acuity measurement using a logMAR chart (Lighthouse, Inc., New York, NY, USA), slit-lamp examination (Model BQ 900; Haag-Streit, Bern, Switzerland), stereoscopic optic disc examination with a 78-diopter lens (Volk Optical, Inc., Mentor, OH, USA) and IOP measurement with a Goldmann applanation tonometer (Haag-Streit). IOP measurements were recorded while the subjects were on their existing medical therapy. AL and central anterior chamber depth (ACD) were measured by IOLMaster (Carl Zeiss, Jena, Germany). Gonioscopy was performed in the dark by fellowship-trained glaucoma specialists (AN and TS) using a Goldmann two-mirror lens at high magnification (×16). Indentation gonioscopy with a Sussman four-mirror lens was used to establish the presence or absence of peripheral anterior synechiae (PAS). An eye was considered to have angle closure if the posterior pigmented trabecular meshwork was not visible for at least 180° on nonindentation gonioscopy with the eye in the primary position. Automated perimetry (24-2 Sita Standard strategy, Humphrey Visual Field Analyzer 750i; Humphrey Instruments, Dublin, CA, USA) was performed on two different occasions.

Glaucoma was defined as the presence of glaucomatous optic neuropathy (GON, defined as loss of neuroretinal rim with a vertical cup-to-disc ratio of >0.7 and/or notching attributable to glaucoma) with a corresponding visual field defect. The visual field defect had to meet the following criteria: (1) glaucoma hemifield test (GHT) outside normal limits, (2) a cluster of three or more, nonedge, contiguous points on the pattern deviation plot, not crossing the horizontal meridian with a probability of <5% being present in age-matched normals (one of which was <1%), and (3) pattern standard deviation (PSD) <0.05; these had to be repeatable on two separate occasions. PACG was defined as the presence of GON with visual field changes as stated above in association with a closed angle (presence of at least 180° in which the posterior trabecular meshwork was not visible on nonindentation gonioscopy), and raised IOP and/or PAS (defined as abnormal adhesions of the iris to the angle that were present to the level of the anterior trabecular meshwork or higher). All subjects with PACG had undergone a laser iridotomy at least 1 month before enrollment in the study.

POAG was defined as GON (defined above) with visual field defects as stated above, raised IOP (IOP >21 mm Hg), and open angles on gonioscopy with no obvious secondary cause for the glaucoma. Normals were defined as having IOP ≤21 mm Hg with open angles, healthy optic nerves, and normal visual fields. Subjects with a history/evidence of previous acute angle closure attacks, intraocular surgery, laser iridoplasty or trabeculoplasty, pseudoexfoliation or pigment dispersion syndrome, and medical therapy that could affect the iris or angle configuration at the time of the study were excluded. Iris tissue obtained from peripheral iridectomy was transferred to a container with BSS/RNAlater. Iris specimens from nine PACG, nine POAG, and five normal control eyes were used for AFM analysis.

Atomic Force Microscopy

The iris samples were transported and tested within 12 hours postoperatively. The iris was first carefully flattened using a polydimethylsiloxane (PDMS) block on a piece of adhesive attached to a petri dish. A piece of plastic film with a cutout hole was mounted on top of the iris to secure it in place (Fig. 1). Force measurements were done at room temperature using Nanowizard II BioAFM (JPK Instruments AG, Berlin, Germany). All measurements were done on the anterior surface of the iris tissue sample. The iris samples were immersed in the liquid media (PBS with 0.1% BSA) during force measurements. The probe consisted of a 4.5 μm diameter polystyrene bead attached to a silicon nitride cantilever (Novascan Technologies, Inc., Ames, IA, USA). The spring constants of the cantilever used were determined by the thermal tune method[14] and typically were 0.03 ± 0.003 N/m. A maximum force of 3 nN and loading rate of 5 μm/s were applied. A hundred force-distance curves in an area of 10 × 10 μm and an average of 15 reference areas from each sample were used to estimate the Young's modulus values. At least 1500 force curves were obtained for analysis. These values were calculated for each recorded curve using JPK Data Processing Software (JPK Instruments AG), which uses a Hertz's contact model for spherical indenters (diameter, 4.5 μm; Poisson's ratio, 0.5) fitted to the extend curves.[10,15] To account for heterogeneity within a single sample, data that did not conform to the Hertz's contact model were manually excluded from analysis along with any statistical outliers. The Hertz model approximated the sample as an isotropic and linear elastic solid occupying an infinitely extending half space. The indenter was not deformable and there were no interactions between indenter and sample. Since the iris cross-sections were sufficiently thick (~500 μm),[6] compared to the indentation depths (~1 μm), the probed section could be considered as a semi-infinite substrate. The contact force, F exerted on a sphere indenting a linear elastic and semi-infinite medium is proportional to the power 1.5 of the indentation depth, δ.

$$F = \frac{4\sqrt{R_c}}{3}\frac{E}{1-\nu^2}\delta^{\frac{3}{2}} \quad (1)$$

Therefore, the Young's modulus, E of the sample can be derived using Equation 1 where the extend portion of the force-indentation ($F-\delta$) curves are fitted. R_c is the radius of tip curvature and ν is the Poisson's ratio. The Kruskal-Wallis test was applied to test for intergroup differences and Fisher's exact test was applied to evaluate for sex differences. Intergroup variations in Young's modulus were tested for significant differences and Bonferroni corrections were applied to adjust the P values.

For morphologic characterization, a Dimension Icon AFM (Bruker, Billerica, MA, USA) was used in peak force tapping mode at ambient conditions, to record height and peak force error images at 1 Hz. A ScanAsyst-Air cantilever (Bruker) with nominal spring constant of 0.4 N/m and tip radius of 2 nm was used. Image analysis was performed using Nanoscope v1.7 software (Bruker) where the diameter and the d-spacing of the collagen fibers were measured.

Results

There were no differences in age, sex distribution, or IOP among the three groups (Table 1). The AL and ACD were lower in PACG eyes. The vertical cup-to-disc ratio was higher in the glaucomatous eyes (Table 1). Mean number of glaucoma medications was similar in POAG (1.78 ± 0.40) and PACG (1.67 ± 0.50; $P = 0.62$) eyes. Eight eyes in the PACG group and six in the POAG group were on prostaglandin therapy (88.9% vs. 66.7%; $P = 0.57$).

Table 2 and Figure 2 show the average Young's modulus of the iris with different conditions. The iris from the normal controls had the lowest Young's modulus (0.85 kPa; 95%

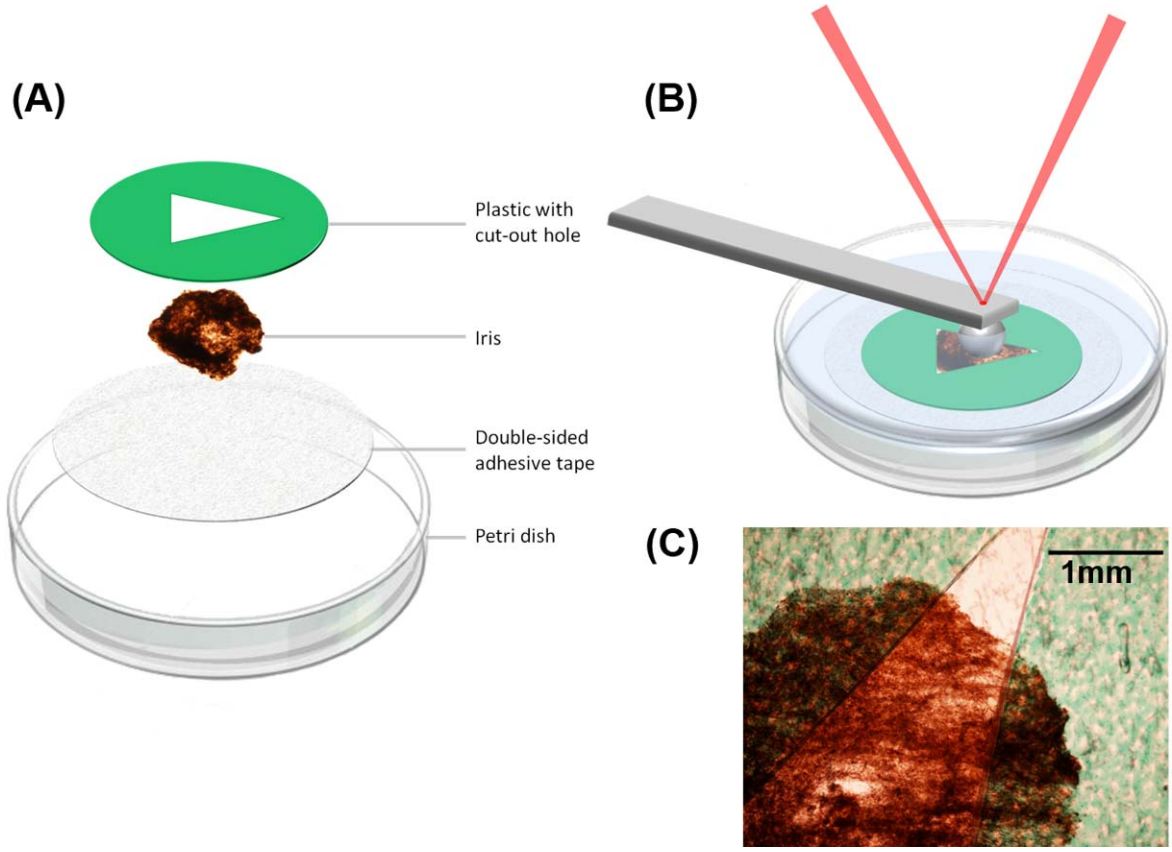

Figure 1. (**A**) Schematic diagram showing the iris sample mounted on a petri dish for AFM measurements. (**B**) AFM cantilever with a 4.5 μm diameter spherical bead was used for stiffness measurements. (**C**) Optical image of a mounted iris sample with the anterior surface exposed.

confidence interval [CI], 0.57–1.11 kPa), while the iris from PACG patients had the highest Young's modulus (2.40 kPa, 95% CI, 1.87–2.94 kPa). The Young's modulus of PACG iris was significantly higher compared to that of the normal controls ($P = 0.005$) and POAG iris ($P = 0.001$). However, there was no significant difference in the Young's modulus of POAG iris compared to that of the normal controls ($P = 0.511$). Figure 3 shows the force-distance curves for the normal, POAG, and PACG irides when the same maximum indentation force of 3 nN was applied. The steepest slope and lowest indentation depth were observed for the PACG iris (black curve). This corresponded to a stiffer material with a larger Young's modulus (E). Figure 4 shows AFM morphologic images of

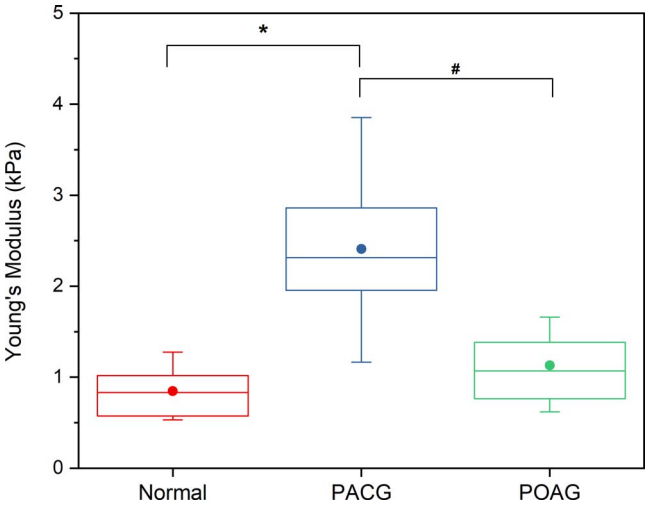

Figure 2. *Box* and *whisker* plots of the Young's modulus of human irides with different conditions. The iris from the normal controls had the lowest modulus (0.85 kPa), while the iris from PACG patients had the highest modulus (2.4 kPa). The Young's modulus of PACG iris was significantly higher compared to the normal controls *($P = 0.005$) and POAG iris #($P = 0.001$). The *box* and *whisker* plots show the mean Young's modulus (*full circle*), median, first and third quartiles (*box*), and range of data (*whiskers*).

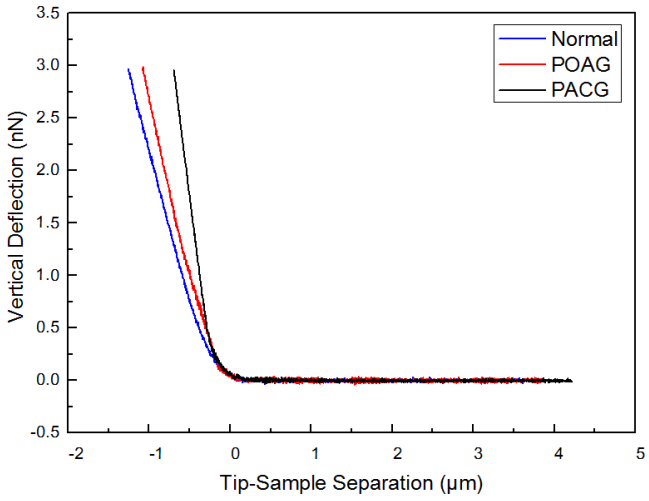

Figure 3. Representative force-distance curves showing different stiffnesses of the human irides.

Table 1. Demographic and Biometric Data

	POAG, $n = 9$	PACG, $n = 9$	Controls, $n = 5$	P
Age, y (SD)*	72.0 (8.6)	70.7 (6.5)	76.4 (11.9)	0.331
Sex, % F	22.2	33.3	0	0.390
IOP (SD)*	18.1 (4.6)	19.2 (7.4)	15.6 (2.6)	0.659
ACD, mm, mean (SD)*	3.3 (0.4)	2.8 (0.3)	3.2 (0.3)	0.023
Axial length, mm, mean (SD)*	25.3 (1.6)	23.4 (0.8)	24.4 (1.6)	0.065
Vertical CD ratio, mean (SD)*	0.89 (0.1)	0.85 (0.1)	0.4 (0.1)	0.011

* Kruskal Wallis and Fisher's exact test for sex.

normal, PACG, and POAG irides. In Figure 4B, inset, the D-period of collagen fibrils with 67 nm bands is clearly visible. This demonstrated the presence of collagen fibrils exposed on all the irides surfaces. Larger diameter collagen fibers also were observed in the PACG iris (Figs. 4C, 4D) compared to normal (Figs. 4A, 4B) and POAG (Figs. 4E, 4F) irides.

Discussion

Few studies to date have explored in vitro testing of iris biomechanical properties. Whitcomb et al.[16] measured the biomechanical properties of porcine iris using microindentation. They found that the posterior components of the iris (namely, dilator fibers, pigment epithelium, and sphincter) were on average stiffer (4.4 kPa) than the anterior stromal layer (2.3 kPa).

Our study is a novel attempt to quantify the in vitro biomechanical properties of human iris as determined by AFM measurements in healthy (normal control) and diseased (PACG and POAG) eyes. The magnitude of the measured Young's modulus of the human iris (0.85–2.41 kPa) was comparable to that of the reported anterior stroma of the porcine iris (2.3 kPa). Our findings of significantly stiffer iris in eyes with PACG compared to normal control and POAG eyes corroborates other imaging[5–7] and histologic studies[8,9] that also reported distinct iris characteristics in different glaucoma subtypes. The iris is considered to have an important role in the pathogenesis of angle closure glaucoma. Anatomic features, such as increased thickness and curvature,[6] as well as dynamic iris movements and changes with pupil dilation[5,7] have been described as possible mechanisms causing angle closure. Furthermore, it has been reported that the collagen components of the iris stroma may have an impact on the biomechanical properties of the iris. Interestingly, genome-wide association studies of PACG found a significant association of PACG with COL11A1, a collagen related gene.[17] Histologic studies conducted by He et al.[9] found that type I collagen and overall collagen density in the iris stroma were greater in acute angle closure eyes compared to normal. Type I collagen is less elastic than Type III (the other major collagen found in iris) and it aggregates to form thick fibers. Their findings suggest that biomechanical properties of the iris may be associated with development of acute episodes of angle closure. In our study, similar observations of larger diameter collagen fibers (167.7 ± 17.8 nm) were observed on PACG iris while normal (77.3 ± 9.9 nm) and POAG (79.6 ± 17.3 nm) irides have predominantly smaller diameter collagen fibers (Fig. 4). Type I collagen fibrils reportedly have diameters ranging from 150 to 300 nm, compared to 25 to 100 nm for Type III collagen fibrils on transmission electron microscopy (TEM) image analysis.[18] This suggests that PACG irides may have a higher density of Type I collagen contributing to the increase in stiffness.

Table 2. Comparison of Young's Modulus in Normal and Diseased Eyes

Groups	Young's Modulus (kPa)	95% CI
Normal, $n = 5$	0.85 ± 0.31	0.57–1.11
PACG, $n = 9$	2.40 ± 0.82*	1.87–2.94
POAG, $n = 9$	1.13 ± 0.36†	0.89–1.37

* $P = 0.005$ vs. normal.
† $P = 0.511$ vs. normal.

Zheng et al.[19] reported the novel associations of a slower speed of iris constriction in eyes with angle closure as well as a lower acceleration of iris stretch, and a more convex iris configuration compared to open-angled eyes, suggesting that such differences in irido-pupillary dynamics may have a role in the pathogenesis of angle closure. Pant et al.[20] evaluated in vivo iris mechanical properties using optical coherence tomography scans and image-based inverse modeling analysis. They found that the irides of patients with a history of PACG were significantly stiffer compared to healthy irides. This corroborates our findings and confirms the association of increased iris stiffness in eyes with PACG. While the exact reasons for the distinctive iris characteristics in angle closure may be many, plausible reasons for a stiffer iris in PACG eyes are due possibly to an increase in collagen density and iris thickness. Furthermore, the standard deviation in the Young's modulus in PACG iris also was the highest. This might result from the increased inherent heterogeneity of the iris tissue in these eyes. We did consider the possibility of the presence of PAS altering the overall biomechanics of the iris. A sub-analysis showed no difference of Young's modulus between eyes with (2.97 ± 0.71 kPa) and without (1.85 ± 0.48 kPa; $P = 0.12$) PAS. Modulus values in angle closure eyes without PAS were persistently higher compared to those of POAG eyes (1.85 vs. 1.13; $P = 0.04$). In summary, the angle closure eyes had higher modulus irrespective of the presence of synechiae; however, we must be aware that the number of eyes in such a subanalysis tends to be small and we must be cautious in extrapolating these findings.

Our study has several limitations. We encountered some difficulties when working with human iris tissue. During our experiments, we noted pronounced adhesion of the posterior iris surface to the AFM tip, presumably due to the presence of pigment epithelium on the posterior surface. This led to difficulty in obtaining indentation measurements. Therefore, indentations were done on the anterior surface of the iris where minimal adhesions were observed in the retract force-distance curves. The ability to concurrently measure the magnitude of the Young's modulus in the posterior surface may yield different estimates that are specific to the region assessed, as observed by Whitcomb et al.[16] and Jouzdani[21] in their experiments on porcine eyes. Jouzdani [21] measured the specific components of the porcine iris and showed that the dilator and sphincter could have a more significant role in determining iris flexibility. In this study, specific regions of the iris could not be tested since relatively small sections of the human irides (<2.0 mm diameter) were obtained from surgery. We should be cautious while

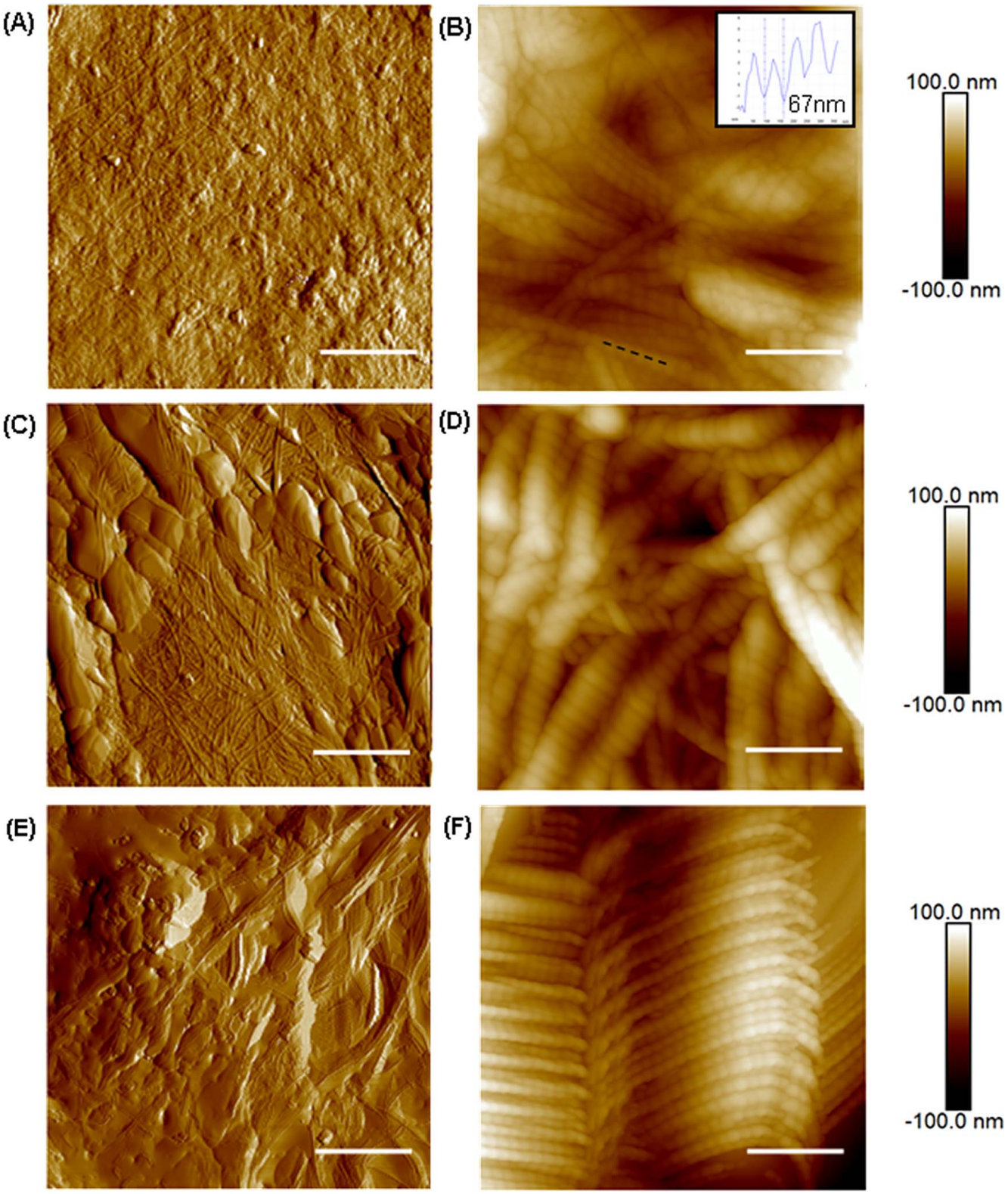

Figure 4. AFM images of collagen fibers from (**A**, **B**) normal, (**C**, **D**) PACG, and (**E**, **F**) POAG irides. Peak force error images are shown in (**A**, **C**, **E**); *scale bar*: 5 µm. Higher magnification height images are shown in (**B**, **D**, **F**); *scale bars*: 0.5 µm. *Inset* in (**B**) shows cross-section of the collagen fiber at the *dotted line*. *Color bar* represents the height of the features.

Investigative Ophthalmology & Visual Science

making these comparisons, since a human iris may differ greatly from a porcine iris and, furthermore, as stated by Mckee et al.,[22] the values of Young's modulus for soft biological tissues depends on the method (indentation versus tensile) by which it is obtained. Hence, we should be aware that modulus values may not be generalized, and it may not be appropriate for predictive models developed previously.[23] A significant proportion of our glaucoma subjects were on prostaglandin analog therapy. Evidence suggests that topical prostaglandins induce increased turnover and remodeling of ECM adjacent to ciliary muscle cells.[24] The increased degradation of ciliary muscle ECM by matrix metalloproteinases has been attributed to the decrease in the hydraulic resistance to uveoscleral outflow.[25,26] This would mean a significant change in the uveal tissue biomechanical properties. Though the proportion of those on prostaglandin therapy was similar between the glaucoma subtypes, it could, however, have influenced the difference in Young's modulus between the normal and glaucoma cases. Finally, tissue properties could be vastly different in in vivo conditions compared to exsanguinated tissues used in the AFM.

In conclusion, we noted stiffer iris in PACG eyes characterized by the estimation of Young's modulus, a measurement of the biomechanical properties of tissues. This suggested that altered biomechanical properties of the iris may have a role in the pathogenesis of PACG. The study further emphasized the fundamental biomechanical and molecular differences in eyes with PACG compared to eyes with POAG. An understanding of this basis creates a new platform to understand disease pathology better and work on therapeutic strategies that will address the same.

Acknowledgments

Supported by New Investigator Grant (2011), Singapore Ministry of Health's National Medical Research Council and Singapore Translational Research Investigator Award (NMRC/STAR/0023/2014) from the Singapore Ministry of Health's National Medical Research Council.

Disclosure: **A. Narayanaswamy**, None; **M.H. Nai**, None; **M.E. Nongpiur**, None; **H.M. Htoon**, None; **A. Thomas**, None; **T. Sangtam**, None; **C.T. Lim**, None; **T.T. Wong**, None; **T. Aung**, None

References

1. Congdon NG, Youlin Q, Quigley H, et al. Biometry and primary angle-closure glaucoma among Chinese, white, and black populations. *Ophthalmol*. 1997;104:1489–1495.
2. Lowe RF. Aetiology of the anatomical basis for primary angle closure glaucoma: biometrical comparisons between normal eyes and eyes with primary angle-closure glaucoma. *Br J Ophthalmol*. 1970;54:161–169.
3. Sihota R, Lakshmaiah NC, Agarwall HC, et al. Ocular parameters in subgroups of angle closure glaucoma. *Clin Exp Ophthalmol*. 2000;28:253–258.
4. George R, Paul PG, Baskaran M, et al. Ocular biometry in occludable angles and angle closure glaucoma: a population based survey. *Br J Ophthalmol*. 2003;87:399–402.
5. Quigley HA, Silver DM, Friedman DS, et al. Iris cross-sectional area decreases with pupil dilation and its dynamic behavior is a risk factor in angle closure. *J Glaucoma*. 2009;18:173–179.
6. Wang B-S, Narayanaswamy A, Amerasinghe N, et al. Increased iris thickness and association with primary angle closure glaucoma. *Br J Ophthalmol*. 2011;95:46–50.
7. Aptel F, Denis P. Optical coherence tomography quantitative analysis of iris volume changes after pharmacologic mydriasis. *Ophthalmol*. 2010;117:3–10.
8. Chua J, Seet LF, Jiang Y, et al. Increased SPARC expression in primary angle closure glaucoma iris. *Mol Vis*. 2008;14:1886–1892.
9. He M, Lu Y, Liu X, Ye T, Foster PJ. Histologic changes of the iris in the development of angle closure in Chinese eyes. *J Glaucoma*. 2008;17:386–392.
10. Last JA, Liliensiek SJ, Nealey PF, Murphy CJ. Determining the mechanical properties of human corneal basement membranes with atomic force microscopy. *J Struct Bio*. 2009;167:19–24.
11. Tijore A, Cai P, Nai MH, et al. Role of cytoskeletal tension in the induction of cardiomyogenic differentiation in micropatterned human mesenchymal stem cell. *Adv Healthc Mater*. 2015;4:1399–1407.
12. Jiang X, Nai MH, Lim CT, Le Visage C, Chan JK, Chew SY. Polysaccharide nanofibers with variable compliance for directing cell fate. *J Biomed Mater Res Part A*. 2015;103:959–968.
13. Hearn EJ. Simple stress and strain. In: *Mechanics of Materials* Vol. 1. 3rd ed. Butterworth-Heinemann; 1997:1–26.
14. Hutter JL, Bechhoefer J. Calibration of atomic-force microscope tips. *Rev Sci Inst*. 1993;64:1868–1873.
15. Sneddon IN. The relation between load and penetration in the axis symmetric boussinesq problem for a punch of arbitrary profile. *Int J Eng Sci*. 1965;3:47–57.
16. Whitcomb JE, Amini R, Simha NK, Barocas VH. Anterior-posterior asymmetry in iris mechanics measured by indentation. *Exp Eye Res*. 2011;93:475–481.
17. Vithana EN, Khor CC, Qiao C, et al. Genome-wide association analyses identify three new susceptibility loci for primary angle closure glaucoma. *Nat Genet*. 2012;44:1142–1146.
18. Asgari M, Latifi N, Heris HK, Vali H, Mongeau L. In vitro fibrillogenesis of tropocollagen type III in collagen type I affects its relative fibrillar topology and mechanics. *Sci Rep*. 2017;7:1392.
19. Zheng C, Cheung CY, Narayanaswamy A, et al. Pupil dynamics in Chinese subjects with angle closure. *Graefes Arch Clin Exp Ophthalmol*. 2012;250:1353–1359.
20. Pant AD, Gogte P, Pathak-Ray V, et al. Increased iris stiffness in patients with a history of angle-closure glaucoma: an image-based inverse modeling analysis. *Invest Ophthalmol Vis Sci*. 2018;59:4134–4142.
21. Jouzdani S. *Biomechanical Characterization and Computational Modeling of the Anterior Eye* [dissertation]. Minneapolis, NM: University of Minnesota; 2003:85–117.
22. McKee CT, Last JA, Russell P, Murphy CJ. Indentation versus tensile measurements of Young's modulus for soft biological tissues. *Tissue Eng Part B Rev*. 2011:155–164.
23. Heys JJ, Barocas VH, Taravella MJ. Modeling passive mechanical interaction between aqueous humor and iris. *J Biomech Eng*. 2001;123:540–547.
24. Lindsey J, Kashiwagi K, Kashiwagi F, Weinreb R. Prostaglandin action on ciliary smooth muscle extracellular matrix metabolism: implications for uveoscleral outflow. *Surv Ophthalmol*. 1997;42:S53–S59
25. Weinreb RN, Kashiwagi K, Kashiwagi F, Tuskahara S, Lindsey JD. Prostaglandins increase matrix metalloproteinase release from human ciliary smooth muscle cells. *Invest Ophthalmol Vis Sci*. 1997;38:2772–2780.
26. Ocklind A. Effect of latanoprost on the extracellular matrix of the ciliary muscle: a study on cultured cells and tissue sections. *Exp Eye Res*. 1998;67:179–191.